13th ewtec 2019 Proceedings of the 13th European Wave and Tidal Energy Conference 1-6 Sept 2019, Naples, Italy

Demonstration of blade pitch control for horizontal-axis tidal turbines

Katherine D. Van Ness, Craig S. Hill, Alberto Aliseda, and Brian L. Polagye

***Abstract*— The majority of utility-scale horizontal-axis tidal turbines use speed control or pitch control to maintain power output once the currents exceed a threshold value (the "rated speed") for the device. In this study, we experimentally characterize power performance and structural loading over a wide range of blade pitch settings and tip speed ratios for a three-bladed horizontal-axis turbine. We then implement a control strategy to maintain power output in unsteady currents using blade pitch control and compare its performance and loading profiles against those from overspeed and underspeed control for a fixed pitch turbine. The experiments are conducted with a 0.45-diameter turbine in an open channel flume with 35% blockage. An acoustic Doppler velocimeter was placed 3-diameters upstream of the rotor plane to measure free stream velocity. During pitch characterization experiments, inflow velocity was maintained at 0.8 m/s (Reynolds-independent) with 4% turbulence intensity. A six-axis load cell at the blade root allowed fluctuations in blade loads to be characterized separately from overall loads on the rotor, which were measured by a similar six-axis cell in the rotor hub. To demonstrate the effectiveness of pitch control in maintaining power output in time-varying inflow, a proportional feedback controller actuating blade pitch was implemented in oscillating flow 0.7-0.8 m/s with a 20-minute period and the resulting fluctuations in power and structural loading were recorded. A similar controller actuating rotor speed was also implemented, and the comparison with the pitch controller demonstrates that pitch control substantially reduces torque or thrust relative to underspeed or overspeed control, respectively.**

***Keywords*—Blade pitch control, horizontal-axis turbine, speed control**

This submission (ID 1468 of Tidal device development and testing) was supported by the United States Facilities Engineering Command (NAVFAC).

K. D. Van Ness, A. Aliseda, and B.L. Polagye are with the Mechanical Engineering Department, University of Washington, 3900 E Stevens Way, Seattle, WA (emails: kvanness@uw.edu, aaliseda@uw.edu, bpolagye@uw.edu).

C. S. Hill is with the Department of Mechanical and Industrial Engineering, University of Minnesota Duluth, 1303 Ordean Ct, Duluth, MN 55812 and the Large Lakes Observatory, University of Minnesota Duluth, 2205 E 5th St, Duluth, MN 55812 (email: cshill@d.umn.edu).

I. Introduction

COST and reliability remain some of the major challenges limiting tidal turbine technology from widespread application. Surviving marine environments where loads are significantly greater than in wind contribute to the high cost and shorter life-span of tidal turbines [1]. This, in addition to having an insufficient understanding of the magnitude of hydrodynamic loads on the turbine, results in blade failure or excessive safety factors which both increase costs [2]. Investigating control strategies to help mitigate loading can bring down the cost of the technology and extend the lifespan of the device [3].

When the turbine is operating above the cut-in speed and below the rated speed (commonly referred to as "Region II", shown in Figure 1), the control objective is to maximize the turbine efficiency (ratio of mechanical shaft power to inflow kinetic power). This is commonly achieved by variable speed control to maintain a constant tip speed ratio ($\lambda = \omega R/U_\infty$) corresponding to maximum efficiency, where ω is the rotational speed of the turbine, R is the radius, and U_∞ is the free stream flow upstream of the rotor. However, in increasing inflow above the rated flow speed ("Region III"), efficiency must be precisely decreased to balance the increase in flow speed and maintain the power output of the turbine. In this study, we investigate specifically Region III control, where either variable speed or variable pitch can be used to meet control objectives [4]. These may be combined with passive control

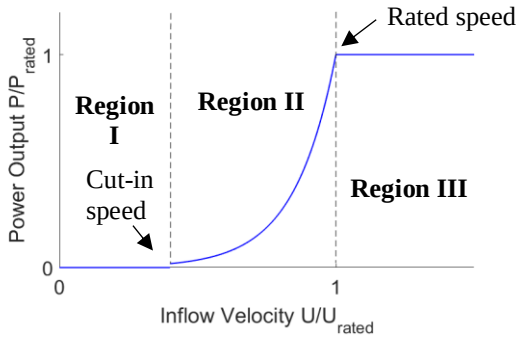

Fig. 1. Typical power curve of operating regions for a tidal turbine.

techniques, such as utilizing the bend-twist coupling of composites [5,6].

Variable speed control strategies are classified as "overspeed" or "underspeed" relative to the rotational speed corresponding to maximum efficiency. Overspeed control involves decreasing generator torque to increase the speed of the rotor such that it surpasses the optimal λ to decrease efficiency. Since thrust coefficient and number of operating cycles increases with λ, the drawback of this strategy is that it leads to high fatigue loads and higher material costs for blade manufacturing [7]. Underspeed control involves increasing generator torque to decrease the speed of the rotor such that it falls below optimal λ and decreases efficiency. Lower λ corresponds to lower thrust on the turbine but a much higher torque to maintain power. When put into practice, this can substantially increase the generator size and cause fluctuating lift and drag forces as more of the blade span enters stall [4]. Alternatively, pitch control relies on changes in blade pitch for reduced C_P and can avoid high thrust and torque loads. However, installation of pitch actuators introduces additional modes of failure, where accessibility to the turbine for maintenance or repairs is already difficult and expensive; this persuades many tidal turbine manufacturers to opt out of variable-pitch and take the consequences in load from speed control [8]. A more quantitative analysis of performance implications of speed and pitch control is needed to inform cost-benefit analysis for variable pitch mechanisms.

To date, pitch control performance for current turbines in Region III have been primarily evaluated in simulation [9,10]. While established methods and new demonstrations of pitch control strategies for wind turbines [11,12] can serve as an appropriate guide for building similar strategies for tidal devices, experimental studies for tidal devices have been limited to fixed pitch tests for a range of blade pitches, which provide only general performance trends for changes in pitch angle away from the design point [13]. This study compares the implementation of these control methods experimentally and discusses how the results could be used to inform turbine design decisions between variable-pitch and fixed-pitch turbines.

II. Experimental Set Up

A. Scale-model turbine

The lab-scale, horizontal-axis turbine used for these experiments was 0.45 meters in diameter and instrumented with two six-axis load cells. The three-bladed device was designed with variable speed and variable pitch. A Nano25 model load cell (ATI Industrial Automation) was installed at the root of a single blade to measure blade loads and a Mini45 model was installed on the main shaft of the turbine, in the hub, to measure thrust and torque on the rotor (Figure 3). The turbine rotor was integrated with a 5:1 gearbox and LV233 double-shaft stepper motor (Parker Hannifin), with an optical encoder mounted on the rear shaft (Figure 3). The stepper motor allowed for precise control of the rotational speed; encoder measurements verified the rotor speed and provided a means to correct each measurement by azimuthally-dependent tare values acquired in quiescent water.

Additional stepper motors and optical encoders were installed in the hub to individually control the pitch angle β of each blade in increments of 0.125° (Figure 3). Analog temperature sensors in the nose cone and hub cavity monitored temperature fluctuations near the load cells, which had been previously found to be sensitive to changes in internal temperature. Blade geometry, based off the NACA-44 series, is described in [7].

B. Recirculating open-channel flume

Experiments were conducted at the University of Washington in a recirculating open-channel flume with a test section 0.6-meter deep and 0.76-meter wide. This resulted in a blockage ratio (rotor swept area relative to the channel cross-section) of 35%. Two pumps were controlled by a variable frequency drive to maintain a constant free stream velocity up to 0.8 m/s with 4.4% turbulence intensity (Figure 2(a)) during performance characterization of the turbine or to oscillate the current between 0.7 m/s and 0.8 m/s (Figure 2(b)) during implementation of speed and pitch control strategies to mimic low frequency fluctuations such as those experienced during daily tidal cycles. Velocity was measured 3-diameters upstream of the rotor plane using a Nortek acoustic Doppler velocimeter (ADV). Reynolds number, $Re = cU_\infty/\nu$, for the various inflow cases ranged from $1.9 * 10^4$ at 0.7 m/s to $2.2 * 10^4$ at 0.8 m/s, where the mid-span chord length $c = 0.028\,m$ was used for the characteristic length. Water temperature was maintained at 19°C for all experiments.

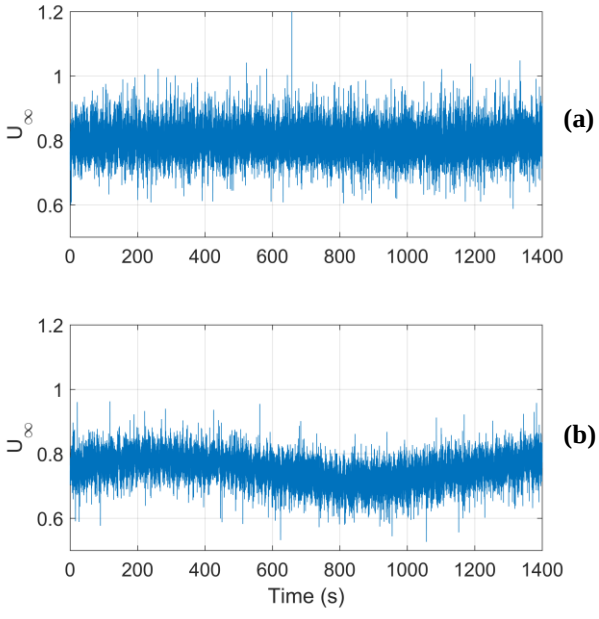

Fig. 2. Sample time series from the ADV during (a) constant inflow averaging 0.8 m/s and (b) oscillating inflow between 0.7 and 0.8 m/s with a 20-minute period.

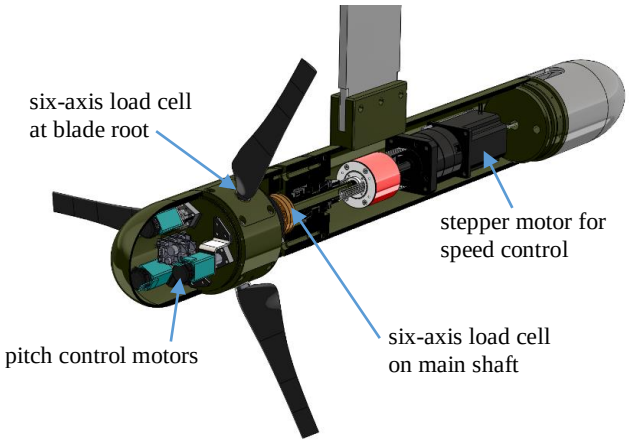

Fig. 3. CAD model of turbine and instrumentation.

C. *Performance characterization*

Prior characterization of turbine performance as a function of blade pitch angle β and tip speed ratio λ demonstrates the motivation for the active pitch control experiments provided in this paper. Operating with the free stream velocity U_∞ shown in Figure 2(a), the power output was calculated from the measured torque τ from the six-axis load cell on the main shaft and rotational speed ω from the stepper motor (verified by the optical encoder) to determine the coefficient of performance:

$$C_P = \frac{\langle \tau\omega \rangle}{0.5\rho A \langle U_\infty^3 \rangle}, \quad (1)$$

where A is the rotor swept area and ρ is the water density. Measured thrust T, also from the hub load cell (and verified by the blade load cell) was used to calculate the coefficient of thrust:

$$C_T = \frac{\langle T \rangle}{0.5\rho A \langle U_\infty^2 \rangle}. \quad (2)$$

In Equations (1) and (2), instantaneous U_∞ was squared or cubed and averaged over the entire test since the free stream flow was constant during performance characterization trials. At each tip speed ratio, instantaneous power and thrust measurements were used to calculate an averaged C_P and C_T over 9000 samples, or several hundred revolutions. Each sample was corrected by the azimuthally-dependent tare values.

Figure 4 shows C_P and C_T as a function of tip speed ratio for a subset of blade pitch angles, where 0° is the design pitch angle. For tip speeds higher than optimal for maximum power production, increasing blade pitch (towards "feather", thus decreasing the angle of attack) decreases the efficiency and thrust, in line with previously reported experimental results [13]. This performance trend is reversed at lower tip speed ratios as increasing pitch moves the point of flow separation along the blade closer to the trailing edge. This result is in line with previous studies (e.g., [14]).

For these experiments, performance was characterized for pitch angles of -5° to +35° in increments of 5° at an inflow velocity of 0.8 m/s. A contour map of interpolated C_P as a function of tip speed ratio and blade pitch is shown in Figure 5(a). A similar map for C_T is shown in Figure 5(b). We can visualize from the contour maps how we might manipulate β or λ to achieve a large range of efficiencies in response to changing inflow.

From the 0° pitch case in Figure 4, we observe that even for $\lambda = 8$, efficiency remains close to optimal and would be insufficient to achieve Region III objectives using overspeed control. Further, physical limitations with the experimental turbine restricts the rotation rate to 5 revolutions per second due to increased friction in the system exceeding the torque limit on the stepper motor at high RPM, so overspeed control was not implemented experimentally. Instead, the experimental pitch and underspeed controllers were compared to an ideal, theoretical overspeed controller.

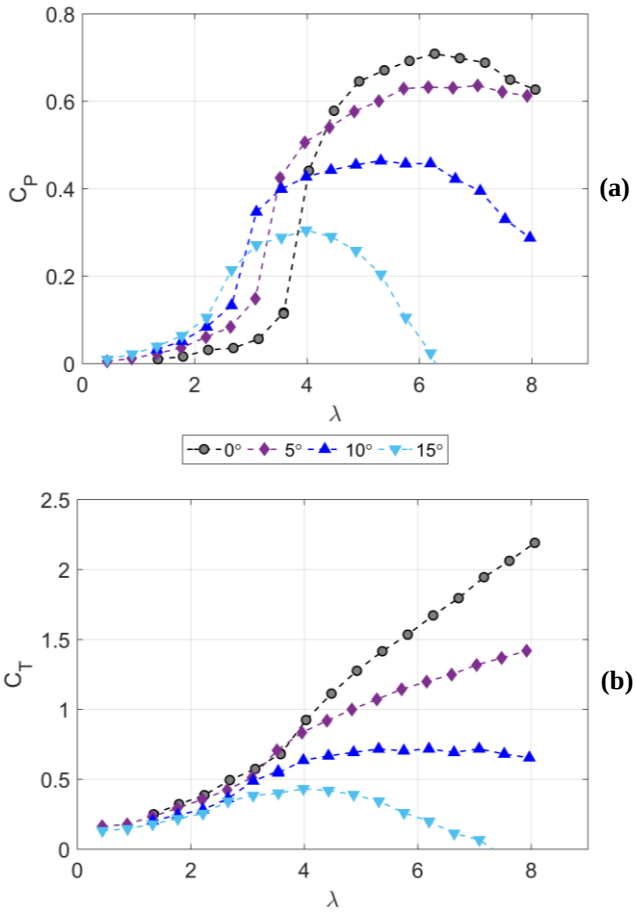

Fig. 4. Coefficients of (a) performance and (b) thrust as a function of tip speed ratio (λ) for various blade pitch settings at 0.8 m/s inflow velocity. 0° is the optimal pitch angle.

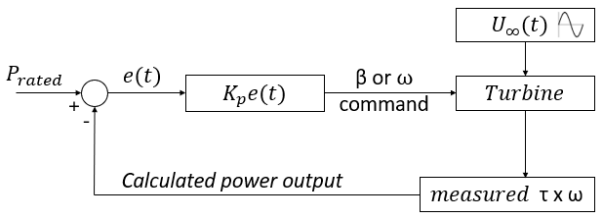

Fig. 6. Proportional controller block diagram.

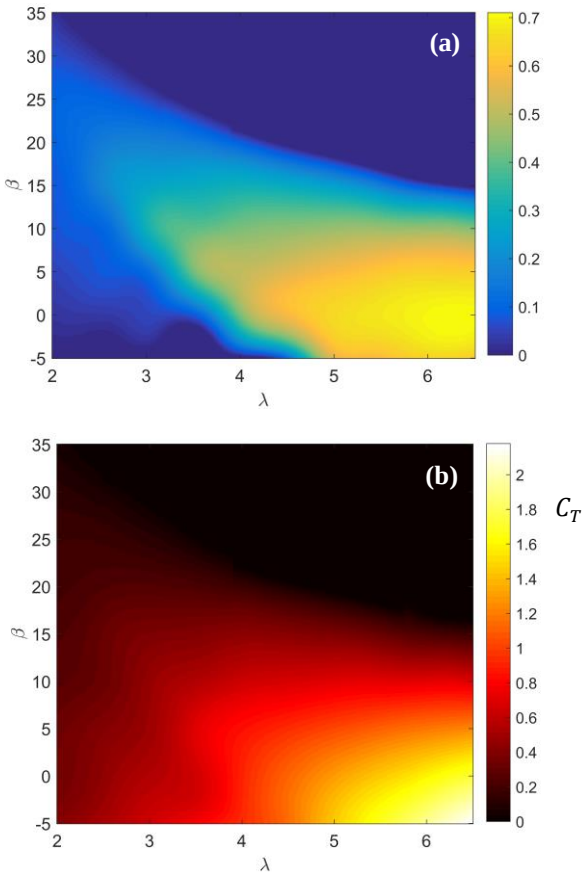

Fig. 5. (a) C_P and (b) C_T contour maps as a function of tip speed ratio (λ) and blade pitch (β) in 0.8 m/s inflow.

D. *Region III Control Strategies*

For these experiments, Region III proportional controllers on mechanical power were used to modulate rotational speed or blade pitch. The rated operating condition perturbed by the control strategy was the rotational speed corresponding to maximum efficiency for the 0° pitch case at the rated speed of 0.7 m/s. Pitch control actuated blade pitch towards feather while holding rotation rate constant. Speed control actuated rotational speed while holding blade pitch constant. Controller gains in all three cases were chosen using *ad hoc* tuning techniques. A proportional gain was sufficient in this set up to maintain power output, although future control versions may include integral or derivative gain, or non-linear control [15], to further minimize fluctuations. To reduce noise in the input signal to the controller, a moving average filter of 800 samples (~60 revolutions) was applied to the measured power (i.e., $\tau\omega$). As shown in Figure 6, the controller input is the error between the power output and the specified rated power of the turbine, P_{rated}. The selected gains for each controller were $K_P = 2.5 * 10^{-4}$ for the speed control case and $K_P = 0.5$ for the pitch control case. To compare the three control strategies, the oscillating inflow from Figure 2(b) was controlled during each experiment while the controller response and corresponding structural loads were observed.

To confirm that the controllers were effective in maintaining the rated power, the standard deviations of the measured power output from the setpoint are compared between the pitch and underspeed controller. The controller performance itself beyond the basic objective of maintaining the rated power was not a focus of this study.

To compare the effects of the controller type on the turbine loads in Region III, thrust and torque were measured from the hub load cell during each control case and plotted with the oscillating inflow velocity, calculated power output, and controlled speed or pitch over a single period. The power was normalized with the reference ("rated") power of 18.4 W (i.e., power at 0.7 m/s at optimal tip-speed ratio for 0° pitch). Thrust and torque were normalized using measured thrust and torque values corresponding to the operating condition where the turbine enters Region III. For the theoretical, ideal overspeed controller, the required efficiency was calculated at each point in the time series and the corresponding thrust and torque values were determined from the performance curves in Figure 4 for the 0° case.

In the underspeed and pitch control cases, the streamwise blade root force measured by the second load cell at the blade root verified the hub thrust measurement within ±5%, where roughly 5% of the blade load was absorbed by the rubber seal surrounding the blade root due to compression during the test.

III. RESULTS

E. *Power fluctuations*

Both the pitch and underspeed controllers succeeded in maintaining power with a standard deviation of 0.5 W around the setpoint of 18.4 W (3% error). Controller ability to maintain power can be seen visually in the time series of the oscillating inflow measured from the ADV (Figure 7(a)) and calculated power output relative to the rated power (Figure 7(c)) for all three controllers. The actuated speed or pitch output from the controller is shown in Figure 7(b).

F. *Hydrodynamic loads*

Figure 7 shows the time series of oscillating inflow, calculated power output, controlled speed or pitch, and

C_P

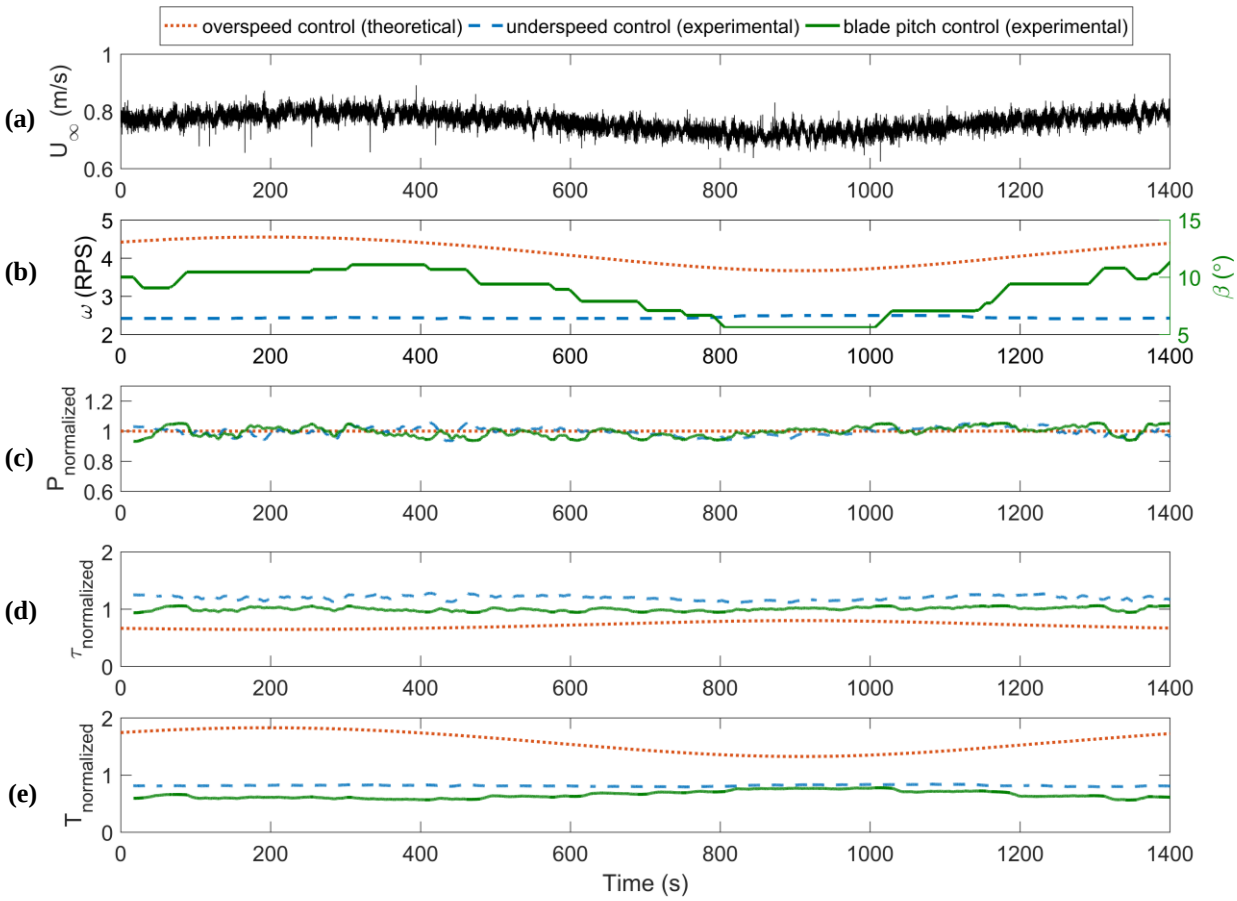

Fig. 7. Time series for (a) free stream velocity, (b) power output relative to the rated power, (c) rotor speed (left axis for speed control cases) or blade pitch (right axis for pitch control), (d) normalized rotor torque, and (e) normalized rotor thrust for overspeed, underspeed, and pitch control. The overspeed case is a theoretical output based on the same velocity inflow and performance curves from Figure 4.

normalized thrust and torque compared for all three controllers. As expected, we observed that between the speed control cases, operating in an overspeed mode reduced torque while dramatically increasing thrust and vice versa for underspeed control. It should be noted that because of the steep drop-off in efficiency at tip-speed ratios below the rated condition (observed in Figure 4(a)), only slight changes in rotational speed were required from the underspeed controller and appear almost constant in the time series in Figure 7. Since the pitch controller maintained constant rotational speed during the test, the measured torque stayed constant to keep power output constant, while spending the duration of the test pitched towards feather significantly reduced the measured thrust on the rotor and blades. This is a realization of the trend shown in Figure 4, where we see that increasing the pitch at constant speed decreases C_P and C_T. By this, the pitch controller avoids both extremes in torque and thrust loads, maintaining a steady torque load while also reducing the thrust well below the rated condition at the entrance of Region III. A summary of the average changes in torque and thrust from the rated condition for each control case is provided in Table 1.

To confirm that the theoretical overspeed values would serve as a suitable comparison, a theoretical underspeed controller was compared with the experimental result. The mean change in torque and thrust for the theoretical underspeed controller was +18.5% and -18.5% compared to the experimental result of +20% and -19% reported in Table 1. Consequently, the theoretical overspeed results are likely similar to what would be observed experimentally.

IV. Discussion

G. *Reynolds number effects*

While the experimental results provided in this study demonstrate and quantify load reduction using blade pitch control in a Reynolds-independent regime, it is also

TABLE 1
MEAN CHANGES IN TORQUE AND THRUST FROM THE RATED CONDITION FOR EACH CONTROLLER

Controller	Mean change in torque from rated condition	Mean change in thrust from rated condition
Overspeed (theoretical)	**-29%**	**+58%**
Underspeed (experimental)	**+20%**	**-19%**
Pitch (experimental)	**0%**	**-34%**

useful to consider how the performance implications of the controller might change for flow speeds below Reynolds independence. In lower flow speeds, turbine performance and hydrodynamic loading become a function of tip speed ratio, blade pitch, *and* Reynolds number, so relative changes in thrust and torque with blade pitch are likely accentuated. In this Reynolds-dependent regime, increases in flow results in operating at higher power and thrust coefficients, but the pitch controller can counteract this by extending the pitch range to move to lower power and thrust coefficients. Ultimately, the advantages and disadvantages of each controller will be exacerbated, thus increasing the relative benefit of pitch control.

H. Blockage effects

Turbine performance in this study is affected by the relatively high blockage ratio of 35% in the test section. Blockage limits fluid expansion around the turbine, resulting in more fluid flow through the rotor plane and, thus, higher measurements of thrust and power than would be observed in an unconfined channel [16]. Because all experiments were conducted at the same blockage ratio, this does not affect the controller performance comparisons made here. However, because equivalent unconfined performance depends on the blockage ratio and rotor thrust [17], and the rotor thrust varies with control scheme, the absolute differences between control schemes is likely dependent on blockage in the operational setting.

I. Choice of Region III controller

Variable pitch demonstrates the best Region III performance in terms of thrust and torque. We also note that in this case, the loads reported in Table 1 are for flows up to 15% above the rated flow for the turbine; a relatively small increase relative to a real turbine. However, the performance of pitch control comes with the cost and complexity of the design and maintenance of pitch control mechanisms. While it is likely less costly than overspeed control which requires the blades and support structures to resist greater loads, pitch control may be similar in cost to underspeed control which requires only a moderate increase in generator size to accommodate increased torque loads (corresponding to elevated electrical current). The range of flow speeds encountered by a turbine will determine the benefit of pitch control relative to underspeed control.

Further applications of variable-pitch that should be considered, and will be explored with this device in future work, are in reducing fatigue loads with intracycle control and combining active pitch control with speed control and/or passive blade pitch control.

V. CONCLUSION

While Region III pitch control is standard practice in wind turbine design, it is not uniformly employed by tidal turbines. Experiments were conducted with a scale-model turbine in oscillating inflow to mimic low-frequency fluctuations above the rated inflow speed for the turbine. Proportional underspeed and pitch controllers were implemented experimentally to maintain a steady power output while observing the hydrodynamic loading on the turbine measured by a load cell on the rotor shaft. The experimental control strategies were compared to the hydrodynamic loading resulting from a theoretical, ideal overspeed controller.

Results demonstrate the benefit of pitch control in significantly reducing the thrust and torque relative to speed control strategies which inherently require an increase in thrust or torque to achieve the desired efficiency for maintaining power. Pitch control, instead, maintains a constant speed while decreasing the angle of attack to shed power, thus avoiding increases in thrust and torque. These results are demonstrated for Reynolds-independent flow regimes, while performance implications in Reynolds-dependent flow are expected to be more significant and increase the benefit of pitch control over speed control. Ultimately, controller selection requires considering costs and benefits of control strategy. The structural loading required for overspeed control suggests this will not be a viable control strategy for most tidal turbines, but the choice between pitch and underspeed control may be more subtle.

ACKNOWLEDGEMENT

Funding was provided by the United States Facilities Engineering Command (NAVFAC). Additional thanks to Justin Burnett for ongoing contributions to this project.

REFERENCES

[1] O'Rourke, F., Boyle, F., Reynolds, A.: Marine current energy devices: Current status and possible future applications in Ireland. Renewable and Sustainable Energy Reviews, 2010. 14(3): p. 1026-1036.

[2] Milne, I.A.; Day, A.H.; Sharma, R.N.; Flay, R.G.L. The characterization of the hydrodynamic loads on tidal turbines due to turbulence. *Renewable and Sustainable Energy Reviews*, 2016. 56: 851-864

[3] Milne, I.A.; Day, A.H.; Sharma, R.N.; Flay, R.G.L. Blade loading on tidal turbines for uniform unsteady flow. *Renewable Energy*, 2015. 77:338-350.

[4] Arnold, M., Biskup, F., Wen Cheng, P. Load reduction potential of variable speed control approaches for fixed pitch tidal turbines. *International Journal of Marine Energy*, 2016. 15:175-190.

[5] R.B. Barber, C.S. Hill, P.F. Babuska, R. Wiebe, A. Aliseda, and M. Motley, "Flume-scale testing of an adaptive pitch marine hydrokinetic turbine," *Composite Structures*, vol. 168, pp. 465–473, 2017.

[6] Nichols-Lee, R.F., Turnock, S.R., Boyd, S.W. Application of bend-twist coupled blades for horizontal axis tidal turbines. *Renewable Energy*, 2013. 50:541-550.
[7] Zhou, Z., Scuiller, F., Charpentier, J.F., Benbouzid, M.E.H., Tang, T. Power control of a nonpitchable PMSG-based marine current turbine at overrated current speed with flux-weakening strategy, *IEEE Journal of Oceanic Engineering*, 2014. 99: 1–10.
[8] Zhou, Z., Benbouzid, M., Charpentier, J., Scuiller F. Developments in large marine current turbine technologies – a review. *Renewable and Sustainable Energy Reviews*, 2017. 71: 852-858.
[9] Gu, Y., Lin, Y., Xu, Q., Liu, H., Li, W., Blade pitch system for tidal current turbines with reduced variation pitch control strategy based on tidal current velocity preview, *Renewable Energy*, 2018. 115:149-158.
[10] Whitby, B. and Ugalde-Loo, C.E. Performance of pitch and stall regulated tidal stream turbines. *IEEE Transaction on Sustainable Energy*, 2014. 5:64-72.
[11] Laks, J.H., Pao, L.Y., Wright, A.D. Control of Wind Turbine: Past, Present, Future. *IEEE Xplore*, 2009. https://ieeexplore.ieee.org/abstract/document/5160590.
[12] Bossanyi, E.A., Fleming, P.A., Wright, A.D. Validation of individual pitch control by field tests on two- and three-bladed wind turbines. *IEEE Transactions on Control Systems Technology*, 2013. 21(4):1067-1078.
[13] Bahaj, A.S.; Molland, A.F.; Chaplin, J.R.; Batten, W.M.J. Power and thrust measurements of marine current turbines under various hydrodynamic flow conditions in a cavitation tunnel and a towing tank. *Renewable Energy*, 2007. 32:407–426.
[14] Gaurier, B., Germain, G., Facq, J.V., Johnstone, C.M., Grant, A.D., Day, A.H., Nixon, E., Di Felice, F., Costanzo, M. Tidal energy "Round Robin" tests comparisons between towing tank and circulating tank results. *International Journal of Marine Energy*, 2015. 12:87–109.
[15] Forburch, D., Cavagnaro, R., Polagye, B. Power-tracking control for cross-flow turbines. *Journal of Renewable and Sustainable Energy*, 2019. https://doi.org/10.1063/1.5075634.
[16] Whelan, J.I., Graham, J.M.R., Peiro, J. A free-surface and blockage correction for tidal turbines. *Journal of Fluid Mechanics*, 2009. 624:281-291.
[17] Barnsley, M.J., Wellicome, J.F. Final Report on the 2nd phase of development and testing of a horizontal axis wind turbine test rig for the investigation of stall regulation aerodynamics. Technical report E.5A/CON5103/1746. 1990.